Biochemical and Biophysical Research Communications 726 (2024) 150306

Contents lists available at ScienceDirect

Biochemical and Biophysical Research Communications

journal homepage: www.elsevier.com/locate/ybbrc

Structural identification and comprehension of human ALDH1L1-Gossypol complex

Chang Woo Han [a,1], Han Na Lee [b,1], Mi Suk Jeong [a], Hong Yeoul Kim [c], Se Bok Jang [b,*]

[a] Institute of Systems Biology, Pusan National University, Jangjeon-dong, Geumjeong-gu, Busan, 46241, Republic of Korea
[b] Department of Molecular Biology, College of Natural Sciences, Pusan National University, 2, Busandaehak-ro 63beon-gil, Geumjeong-gu, Busan, 46241, Republic of Korea
[c] Elysiumbio Inc #2007, Samsung Cheil B/D, 309 Teheran-ro, Gangnam-gu, Seoul, 06151, Republic of Korea

ARTICLE INFO

Keywords:
Cell metabolism
Cryo-electron microscopy
hALDH1L1
Gossypol

ABSTRACT

The folate metabolism enzyme ALDH1L1 catalyzed 10-formyltetrahydrofolate to tetrahydrofolate and CO_2. Non-small cell lung cancer cells (NSCLC) strongly express ALDH1L1. Gossypol binds to an allosteric site and disrupts the folate metabolism by preventing $NADP^+$ binding. The Cryo-EM structures of tetrameric C-terminal aldehyde dehydrogenase human ALDH1L1 complex with gossypol were examined. Gossypol-bound ALDH1L1 interfered with $NADP^+$ by shifting the allosteric site of the structural conformation, producing a closed-form $NADP^+$ binding site. In addition, the inhibition activity of ALDH1L1 was targeted with gossypol in NSCLC. The gossypol treatment had anti-cancer effects on NSCLC by blocking NADPH and ATP production. These findings emphasize the structure characterizing ALDH1L1 with gossypol.

1. Introduction

ALDH1L1 (aldehyde dehydrogenase 1 family member L1), a folate enzyme in one-carbon metabolism, is involved in the one-carbon metabolism, including *de novo* nucleotide biosynthesis, cellular methylation, and generation of NAD(P)H [1–4]. The destruction of one-carbon metabolism dramatically affects cells, reducing cellular proliferation and harming cell division [1–4]. Highly proliferating cells, e.g., cancer, require large amounts of adenosine triphosphate (ATP) and exogenous amino acids for optimal growth. An exponentially growing cell is inverted to fulfill, exciting the cellular metabolism, including oxidative phosphorylation and anaplerotic reaction [3,5]. Cancer cells cannot survive the glycolysis production of ATP. Therefore, glycolysis is unable to meet the energy supply in cancer cells. The importance of non-essential amino acids (NEAA) is involved in various other biosynthesis, including the supply of carbon and nitrogen for the synthesis of other amino acids, nucleic acid [5]. Serine, an NEAA, is required for many biosynthesis, including the synthesis of glycine and cysteine and the production of the phospholipids phosphatidylserine, phosphatidylethanolamine, and sphingomyelin [6]. Metabolic studies showed that one-carbon units derived from serine could be diverted to glycine [7,8]. In addition, cytosolic serine metabolized mitochondrial serine hydroxymethyltransferase 2 (SHMT2) transfers the β-carbon to tetrahydrofolate (THF), generating 5,10-methylene-THF [5]. Next, the one-carbon cycle step generating NADPH is the oxidation of 5,10-methylene-THF. Methylenetetrahydrofolate 1 (MTHFD1) is requires Mg^{2+} and $NADP^+$ for oxidation [9,10]. The cytosolic MTHFD1 or mitochondrial MTHFD2 is a bifunctional enzyme incorporating methylenetetrahydrofolate dehydrogenase and cyclohydrolase [9,10]. As the first step, Mg^{2+} binds to MTHFD1, followed by generated 5,10-methyl-THF and NADPH. Adding a nucleophile (e.g., water) for the cyclohydrolase activity forms a hydrated imidazoline ring [9,10]. The NADPH-producing step is indicated that THF pools in the cytosolic and mitochondrial by 10-formyl-THF dehydrogenase (e.g., ALDH1L1 and ALDH1L2). The FDH (ALDH1L1, EC 1.5.1.6) substrate, 10-formyltetrahydrofolate (10-formyl-THF), is a formyl donor in the biosynthesis step that includes *de novo* purine synthesis. FDH catalyzes the conversion of 10-formyl-THF to THF, C O_2, and NADPH using one-carbon units. FDH is strongly expressed in the liver and activates *de novo* purine nucleotide synthesis and kidney [11]. Previous studies showed that human FDH cDNA suggested a protein comprising 902 amino acids with a molecular weight of 98.7 kDa [12]. The FDH domains are divided into an N-terminal folate-binding domain (aa. 1–310), an intermediate

* Corresponding author.
E-mail address: sbjang@pusan.ac.kr (S.B. Jang).
[1] These authors contributed equally to this article.

https://doi.org/10.1016/j.bbrc.2024.150306
Received 19 June 2024; Received in revised form 20 June 2024; Accepted 21 June 2024
Available online 22 June 2024

domain (aa. 311–419), and an aldehyde dehydrogenase-like C-terminal domain (aa. 420–902) [12].

The Nt-FDH is included in the folate-binding site and hydrolase activity, and catalytically conserved residues, aspartate 142 and histidine 106, have been identified in active sites [13]. Ct-FDH of another site performing a role contains the NADP-binding subdomain, catalytic sub-domain, and an oligomerization sub-domain. The above two-residue necessary catalysts indicated the involvement of cysteine 707 and glutamine 673 [14]. Furthermore, several studies suggested that the ALDH1L1 level increases in lung adenocarcinoma (LUAD), lung squamous cell carcinoma (LUSC), non-small cell lung cancer, and glioblastoma [15–19].

Gossypol, a terpenoid aldehyde, is extracted from cottonseed. It is used as a male contraceptive in Chinese medicine [4,20]. Most studies on Gossypol suggested that this is involved in antitumor activity on human non-small cell lung cancer, breast adenocarcinoma, and glioblastoma [2,19,21]. Most gossypol papers assessed its cancer therapy potential, but the potency of Gossypol in cancer therapy was unsuccessful. Gossypol inhibits ALDH1L1, and is effective in NSCLC cell lines and mouse xenograft models. This paper reports that Gossypol inhibits ALDH1L1 in NSCLC cell lines.

2. Materials and methods

2.1. Purification of human ALDH1L1

The ALDH1L1 (amino acids 1–902) gene was cloned into pET23b and transfected into BL21 (DE3) cells. Cells were sonicated in lysis buffer [50 mM Tris-HCl (pH 7.82), 200 mM NaCl, 1 mM 1,4-dithiothreitol, 10 % glycerol, 1 % Triton X-100, 1 mM sodium azide, and a protein inhibitor cocktail]. The supernatant was loaded onto a Ni-NTA column (Bio-Rad), washed, and the protein eluted with elution buffer [50 mM Tris-HCl (pH 7.82), 200 mM NaCl, 1 mM sodium azide, 1 mM 1,4-dithiothreitol, 10 % glycerol, and 100–200 mM imidazole].

2.2. Biacore surface plasmon resonance (SPR) measurement

The apparent dissociation constant (K_D) between human ALDH1L1 and gossypol was measured using a Biacore T200 biosensor. ALDH1L1 protein in 10 mM acetate buffer (pH 5.0) was coupled to a CM5 sensor chip using the NHS linking method. Kinetic parameters were measured at room temperature using a flow path with ALDH1L1-immobilized and underivatized chips. Gossypol concentrations (62–500 μM) were prepared in HBS buffer and injected at 30 μL/min.

2.3. Vitrobot condition

Three microliter drops of purified ALDH1L1 (8 mg/mL) and 1 mM gossypol were placed on glow-discharged R2/2 Quantifoil holey grids (200 mesh). The protein was blotted for 4 s with a blotting force of −1, with a 20-s waiting time in 100 % humidity at 4 °C. Subsequently, the protein was plunge-frozen in liquid ethane using a Vitrobot 4 (Thermo Fisher Scientific, USA).

2.4. Single particle cryo-EM data collection and image processing

Cryo-EM images of the ALDH1L1-gossypol complex were acquired using a Glacios cryo TEM 200 keV microscope (Thermo Fisher Scientific, USA) equipped with a Falcon III direct detector in electron-counting mode at the KAIST Analysis Center for Research Advancement (KARA). Image processing of the ALDH1L1-gossypol complex was performed using cryoSPARC Live 3.3.2 on a local workstation [22]. Using the Topaz Extract neural network and positive-unlabeled (PU) learning, 3,107,384 particles were automatically selected. After iterative 2D classification, 2,565,990 particles were chosen for ab initio 3D map generation. The volume was further refined through homogeneous refinement, resulting in 396,292 particle images selected for further processing. The final 3D map, refined using homogeneous and nonuniform refinement in cryoSPARC, achieved a resolution of 4.01 Å as estimated by the gold standard Fourier shell correlation (FSC) method.

2.5. Model building

The atomic model of ALDH1L1, based on the crystal structure of the C-terminal domain of 10-formyltetrahydrofolate dehydrogenase from Rattus norvegicus (PDB ID: 4GO2), was rigid-body fitted into the cryo-EM density of the ALDH1L1-gossypol complex using UCSF Chimera [23]. The structure was refined to the consensus cryo-EM map through iterative rounds of manual model building in COOT [24] until Ramachandran validation criteria were met. The geometry-optimized model underwent global refinement using Phenix [25]. The refined model and corresponding cryo-EM map have been deposited in the PDB and EMDB with codes 7YJJ and EMD-33872, respectively.

2.6. Quantification of ATP levels and cell viability with luminescent assay

The cell viability and ATP quantification were measured using a CellTiter-Gl O^{TM} Luminescent Cell Viability Assay Kit (Promega, UK), a simple and sensitive based on quantifying ATP levels to living cells. Non-small cell lung cancer (NSCLC) cell lines (A549 and H23) (Korean cell line bank, KOR) were seeded into white Corning 96 well flat bottom (Sigma, USA) at a density of 1×10^4 cells in culture RPMI 1640 medium (Welgene, Korea) supplemented with 10 % fetal bovine serum (FBS) and 1 % antibiotics (penicillin), 100 μL per well. After 24h of culture in a plate at 37 °C in a CO_2 incubator, the cells were washed and treated with different Gossypol concentrations.

2.7. Bio-transmission electron microscopy

TEM experiments were carried out at KBSI. ALDH1L1 (1–902) protein, purified, was diluted to varying concentrations. Following rinsing, samples were stained with 2 % (w/v) uranyl acetate. Images were captured using a CCD camera (1k/4k, FEI) operating at 120 kV under low-dose conditions.

3. Results

3.1. Overall structure of ALDH1L1-Gossypol complex

This study examined use of cryo-EM to study ALDH1L1-gossypol complex structures and delineate the interaction of the ALDH1L1 with gossypol and localize the binding sites of potential gossypol. For structural studies, full-length human ALDH1L1 was expressed and purified recombinantly (Supplemental Fig. 1A). TEM image of human ALDH1L1 (Supplemental Fig. 1B). The ALDH1L1 comprised the N-terminal formyltransferase domain (residues 1–302) and the C-terminal aldehyde dehydrogenase domain (residues 405–902), which were connected via the intermediate domain (residues 303–404) (Fig. 1A). An attempt was made to obtain the structure of full-length ALDH1L1 protein, but only the C-terminal aldehyde dehydrogenase domain (residues 405–902). The C-terminal aldehyde dehydrogenase domain contains several structural and functional sub-domains that $NADP^+$-binding domain (residues 405–539, 564–675, and 867–893), a catalytic domain (residues 676–885), and an oligomerization domain (residues 540–563 and 894–902) [26]. A 3D reconstruction of the tetrameric assembly of ALDH1L1 with a global resolution of 4.01 Å was obtained (PDB ID: 7YJJ). ALDH1L1 is a typical Rossmann-fold protein of mixed α/β secondary structures with an $NADP^+$-binding pocket. The c-terminal aldehyde dehydrogenase domain is composed of fifteen α-helices (α1- α15) and sixteen β-sheets (β1- β16) (Fig. 1B). The structure of the complex was modeled using the homology template of the C-terminal domain of

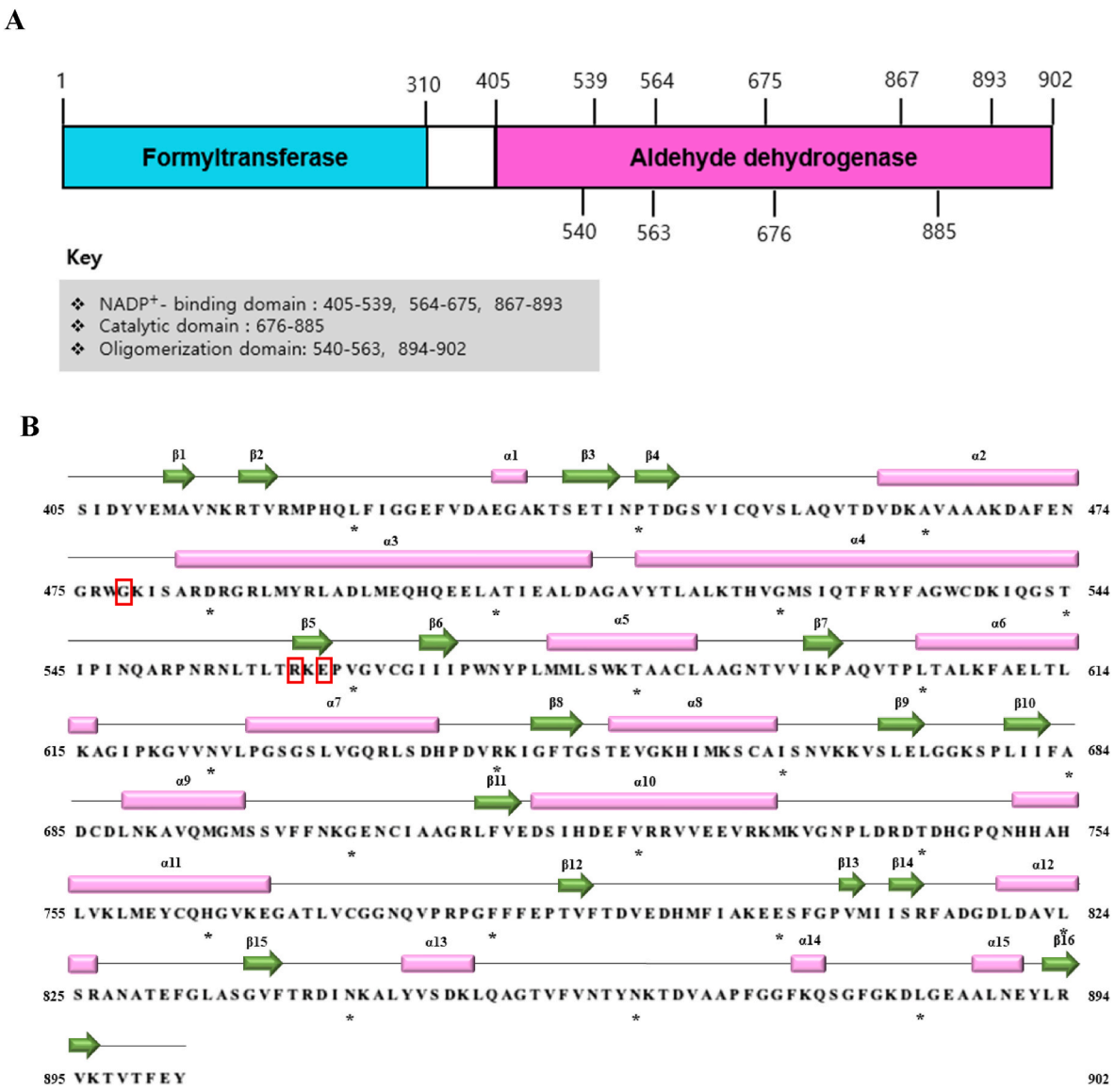

Fig. 1. Schematic representation and biophysical properties of ALDH1L1. (A) Diagram of domain structure of full-length ALDH1L1 (residues 1–902) are shown. (B) The sequence and secondary structure of ALDH1L1. The α-helices are shown as pink, β-sheets as green arrows. * represent mean 20 amino acids section division. (For interpretation of the references to colour in this figure legend, the reader is referred to the Web version of this article.)

10-formyltetrahydrofolate dehydrogenase from *Rattus norvegicus* (PDB ID: 4GO2, 91.80 % sequence identity to human ALDH1L1; Supplemental Fig. 1C). Mus musculus and human ALDH1L1 share 92.35 identical amino acid sequences (Supplemental Fig. 1C). A cryo-EM single-particle dataset was collected and processed, as summarized in Supplementary Table 1. Briefly, 3317 cryo-electron microscopy movies were collected, and 3,107,384 particles were selected for data processing. After 2D classification, ab-initio 3D reconstruction and 3D classification were performed. The complex structure revealed a tetrameric assembly with *C2* symmetry. The structure was fitted as rigid bodies into the cryo-EM map and refined by real-space refinement (Supplemental Fig. 2), resulting in the final model shown in Fig. 2. Fig. 2A presents a surface representation of the ALDH1L1-gossypol complex.

The cryo-EM map unambiguously showed that ALDH1L1 tetramerization is based on the interactions of four subunits to form the catalytic complex of the enzyme [27]. In this structure, the solvent accessible surface area (SASA) of the subunit was subunit A 17809 $Å^2$, subunit B 17616 $Å^2$, subunit C 17809 $Å^2$, and subunit D 18058 $Å^2$. The surface area of 153.803 $Å^2$ was buried in the interface during the complex formation because the surface area of the ALDH1L1-gossypol complex was 71140 $Å^2$.

The structural and biological characteristics of ALDH1L1 suggest that ALDH1L1 has substrate specificities with a strong preference for $NADP^+$ as a coenzyme. The surface representation of ALDH1L1 and gossypol is shown with the acidic region in red, the basic region in blue, and the neutral region in white. The surface of ALDH1L1 indicated that gossypol binds strongly to its basic region, exhibiting a hydrogen connection between the O atom of gossypol and the basic region of ALDH1L1 (Fig. 2B). Gossypol was strongly docked to the β5 (residues G478, R560, and E562) of ALDH1L1 (Fig. 2C and Supplementary Table 2). The binding affinity of ALDH1L1 and gossypol was estimated using the Biacore surface plasmon resonance (SPR). The sensorgrams of gossypol binding to ALDH1L1 were used to calculate the kinetic binding constants. Background sensorgrams were subtracted from the experimental sensorgrams to yield representative specific binding constants. The binding affinity of gossypol for ALDH1L1 was calculated by kinetic analysis of the data using BIAevaluation version 2.1. Gossypol exhibited binding affinities to ALDH1L1, with a K_D (dissociation constant) of 37 μM (Fig. 3A). Moreover, the proposed ALDH1L1-gossypol complex model showed that ALDH1L1 tetramerization is mediated by the C-

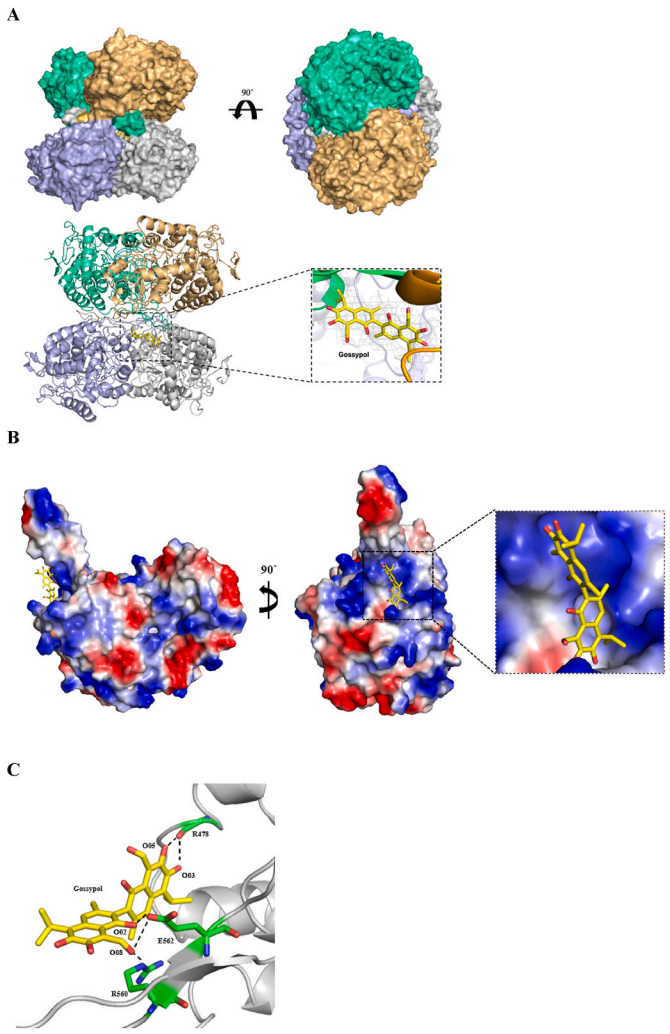

Fig. 2. Structure of the ALDH1L1 and gossypol complex. (A) Ribbon representation of tetrameric structure of c-terminal aldehyde dehydrogenase domain (ALDH1L1) with gossypol (yellow) is shown. (B) The relative distribution of the surface charge of the ALDH1L1 is shown with the acidic region in red, the basic region in blue, and the neutral region in white. (C) Binding region of the ALDH1L1 and gossypol is shown. The gossypol is strongly docking to the residues G478, R560, E562 on β5 of ALDH1L1. (For interpretation of the references to colour in this figure legend, the reader is referred to the Web version of this article.)

terminal assembly of aldehyde dehydrogenase domain to form a novel non-$NADP^+$-binding site; allosteric pocket. Fig. 3B shows the formation of an allosteric pocket in ALDH1L1 due to motion of the four regions: helices E473-A482 (α2-α3), C537-G542 (α4), sheet K/R560-G565 (β5), and loop G591-T593 (near the α5 and β7). In $NADP^+$-bound active state ALDH1L1 (PDB ID: 4GO2), residues from four regions fill the allosteric pocket (Fig. 3C). The major structural deviation occurred around residues E473, N474, G475, R/L476, G478, N481, A482, D538, K539, I540, K/R560, and G565 of the allosteric pocket (Cα RMSD ≧ 1 Å) (Supplementary Table 3).

In contrast to the $NADP^+$-bound active state, gossypol binding can cause conformational modifications of the $NADP^+$-binding pocket. The overall root means square deviation (RMSD) for Cα atoms between the ALDH1L1-gossypol complex and *Rattus norvegicus* ALDH1L1 (PDB ID: 4GO2) was 0.982 Å. The length (Å) between $NADP^+$ and gossypol was 34 Å through WinCoot CCP4 (Fig. 3D). The $NADP^+$-binding pocket constituted the two regions: between the sheet and helix I646-M659 (β8-α8) and loop F700–C707 (near the α9 and β11) (Fig. 3E). In particular, the catalytic cysteine 707 (C707) on the $NADP^+$ binding region is an important residue. The structures of ALDH1L1 with $NADP^+$ exhibited an active open conformation, whereas ALDH1L1 with gossypol showed an inactive, closed conformation (Fig. 3E). The RMSD of $NADP^+$-binding pocket between ALDH1L1- $NADP^+$ and ALDH1L1-gossypol was 0.937 Å. Major structural deviations occurred around residues G647, F648 E653, G655, K656, H657, I658, M659, K703, G704, E705, N70, and C/S707 of the NADP + binding pocket region (Cα RMSD ≧ 1 Å) (Supplementary Table 3).

The $NADP^+$-binding pocket of ALDH1L1 is flexible, existing between two conformational states, usually known as the open or closed. The closed conformation is associated with the inactive conformation, whereas the open conformation is stabilized by $NADP^+$ binding and is essential for enzyme catalysis of ALDH1L1. In contrast, gossypol stabilizes the closed conformation of the $NADP^+$-binding pocket (or active site) and traps the enzyme in an inactive state. Overall, the binding of gossypol to the allosteric pocket of ALDH1L1 structurally disrupts $NADP^+$ binding for the nucleotide-binding site, impairing the ALDH1L1 activity that catalyzes the conversion of 10-formyltetrahydrofolate to tetrahydrofolate and CO_2 (Fig. 4A).

3.2. The cytotoxicity on H23 and A549 cells in combination with gossypol

In most animal cells, ATP is the most common and essential energy molecule for cell growth, division, synthesis, and metabolism. ATP can store or release cellular energy owing to its structural properties of forming high-energy phosphate bonds. Various aspects of the cell metabolism revolve around ATP production and consumption. ALDH1L1 is a folate enzyme that catalyzes the 10-formyltetrahydrofolate (10-CHO-THF) to produce tetrahydrofolate (THF) and CO_2 in an NADP + -dependent reaction. It also regulates reduced folate pools, *de novo* purine biosynthesis, and the flux of folate-bound methyl groups [1].

Cryo-EM structural analysis showed that gossypol binds to the allosteric site of ALDH1L1 and inhibits the $NADP^+$ binding to the enzyme. Based on these results, ALDH1L1-expressing cancer cells were treated with gossypol, and the cell viability was confirmed by measuring the ATP present in the cells in the cell culture state. For the cancer viability quantitation by gossypol inhibition, sensitive and straightforward bioassays were used to determine the number of living cells based on ATP quantitation. ALDH1L1 is overexpressed in NSCLC and catalyzes NADH and ATP [2]. The NSCLC cell lines H23 ($F_{4,5} = 47.82$, $p = 0.0004$) and A549 ($F_{4,5} = 88.53$, $p < 0.0001$), were treated with gossypol and ATP was measured to confirm the inhibitory effects of gossypol in these cell lines. A dose-dependent decrease in ATP production was observed as the gossypol concentration was increased in both H23 and A549 cell lines. The gossypol treatment for 24 h induced cell death and decreased the total ATP by approximately 45–50 % (Fig. 4B). These results show that gossypol binds to the allosteric site of ALDH1L1 and inhibits its catalytic activity.

4. Discussion

ALDH1L1 is a crucial one-carbon reaction folate enzyme in cellular metabolism, including *de novo* nucleotide biosynthesis and cellular methylation. The ALDH1L1 metabolic reaction generated NADPH production, so the catalytic site of the folate enzyme required an NADP cofactor. This study established the allosteric pocket of ALDH1L1 to the binding site of gossypol that impeded NAD P^+ binding to ALDH1L1 owing to structural conformation. The enzyme conserved the cellular THF pool by converting 10-formyl-THF to THF and C O_2 in an NAD P^+-dependent reaction. Therefore, this reaction is related to regulating the purine levels by competing for 10-formyl-THF, which is used for two reactions in the *de novo* purine pathway. The level of ALDH1L1 expression is strong in the liver, the main function of folate metabolism, rather than kidney and pancreas [11,28,29]. A previous study suggested

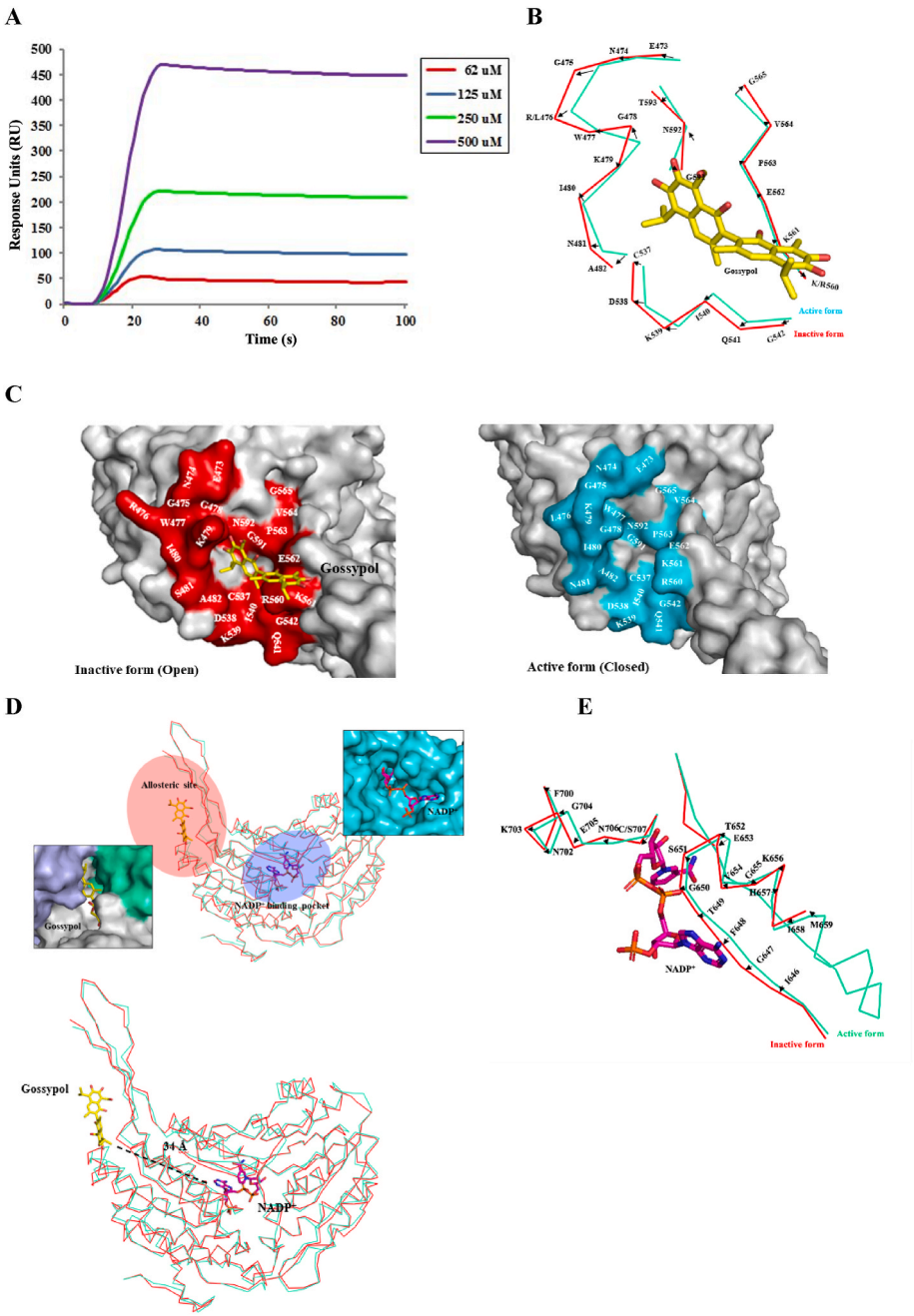

Fig. 3. Schematic representation and biophysical properties of ALDH1L1 and gossypol. (A) Biacore biosensor analysis of ALDH1L1 binding to gossypol at 25 °C. Gossypol sensorgrams for 62, 125, 250, and 500 μM are shown. (B) Superimposition of the Cα chain tracers of the ALDH1L1 [PDB ID: 7YJJ] with gossypol and C-terminal domain of Aldh1l1 from Rattus norvegicus [PDB ID: 4GO2] is shown. (C) Active form is represented $NADP^+$ bound state of Aldh1l1 [PDB: 4GO2]. Inactive form is represented Gossypol bound state of human ALDH1L1 [PDB: 7YJJ]. The allosteric pocket in ALDH1L1 has the four regions (red); α2-α3 helices (E473-A482), α4 helix (C537-G542), β5-sheet (K/R560-G565), and loop near the α5 and β7 (G591-T593). (D) Superposition of the Cα chain tracers of the ALDH1L1 with gossypol (gray) and ALDH1L1 with $NADP^+$ (cyan) is shown. The communication length between gossypol and $NADP^+$ is shown. (E) Superposition of the Cα chain tracers of the ALDH1L1 with gossypol [PDB ID: 7YJJ] and C-terminal domain of Aldh1l1 from Rattus norvegicus [PDB ID: 4GO2] about $NADP^+$ is shown. (For interpretation of the references to colour in this figure legend, the reader is referred to the Web version of this article.)

that ALDH1-positive cells exhibited cancer stem cell properties, in vitro self-renewal, differentiation, and resistance. This study analyzed the expression of ALDH1 for the CSC characteristics in 303 lung tissues from different patients with lung cancer [18]. Further study showed that NSCLC cells increased the expression levels of the ALDH isoforms [30]. Survival analysis revealed a poor survival rate in ALDH1L1-positive patients rather than ALDH1L1-negative patients [18,30].

Gossypol is a terpenoid extracted from cottonseed and is involved as a non-competitive binding of cofactors, such as NAD^+ in ALDH-induced oxidation [4,18]. The exact biological mechanism of inhibition of ALDH1L1 with gossypol is unclear. The structural characteristics and biological potency were observed between ALDH1L1 and gossypol. ALDH1L1 contributed ATP production through NADPH generation and formate depletion in NSCLC cells. Reverse ATP production and NADPH generation are caused by gossypol therapy, which leads to a reduced level of NSCLC (Fig. 4 B). Several studies have shown that H23 and A549 cells strongly express the ALDH1L1 protein [2,17]. According to previous reports, ALDH1L1 is related to ATP production through folate

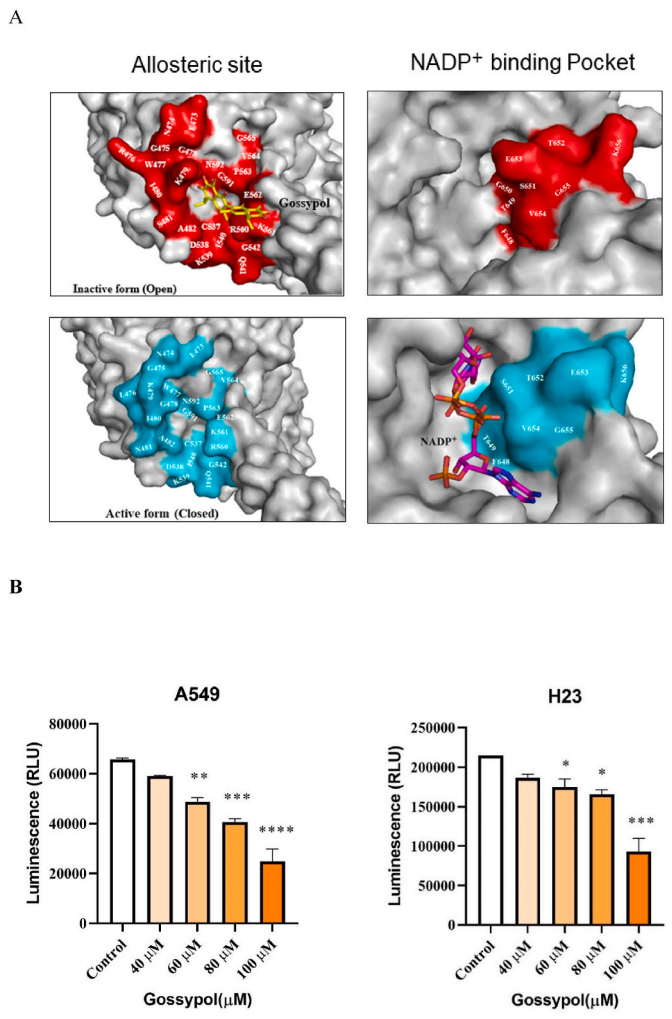

Fig. 4. (A) Comparison of active, inactive, and gossypol-bound conformation of ALDH1L1. A cartoon model of ALDH1L1 in the inactive (up: gossypol bound) and active (down: $NADP^+$ bound) form is shown. The gossypol binds strongly with the ALDH1L1. (B) The inhibitory effect of gossypol about ATP production and cell viability assay. Gossypol was incubated for 24 h in different NSCLC cell lines including A549 and H23. Statistical significance was determined using one-way ANOVA, with Bonferroni's correction. $*p < 0.05$, $**p < 0.01$, $***p < 0.001$ and $****p < 0.0001$ vs vehicle.

metabolism. The folate metabolism is a crucial metabolic pathway for nucleic acid synthesis in a one-carbon metabolism. The folate metabolism in cancer cells is highlighted by NADPH production. In addition, NADPH production is related to methylenetetrahydrofolate dehydrogenase (MTHFD). Therefore, ALDH1L1 could catalyze the 10-formyl-THF, a product of MTHFD oxidation, to produce THF and NADPH [31]. As a result, a treatment with gossypol, an ALDH1L1 inhibitor, decreased ATP synthesis in NSCLCs strongly expressing ALDH1L1 by approximately 50 %. The active situation of ALDH1L1 with $NADP^+$ was examined to compare structural differences for gossypol in ALDH1L1. A novel binding site to gossypol that was distinct from the $NADP^+$ catalytic site was also discovered. As known to the $NADP^+$ binding region, catalytic cysteine 707 (C707) occurred alternatively motion in a gossypol-bound state. Moreover, the allosteric pocket in the gossypol-bound state is represented by the four regions: helices E473–A482, C537–G542, sheet K/R560–G565, and loop G591–T593. This region is a closed allosteric pocket in the $NADP^+$-bound state, opening the allosteric pocket in the free state. As a result, gossypol binds to an allosteric site and disrupts the folate metabolism by preventing $NADP^+$ binding. Finally, the complex between the aldehyde dehydrogenase domain of ALDH1L1 and gossypol disrupts the folate metabolism by blocking $NADP^+$ binding.

CRediT authorship contribution statement

Chang Woo Han: Writing – original draft, Software, Funding acquisition, Data curation. **Han Na Lee:** Writing – original draft, Methodology, Data curation. **Mi Suk Jeong:** Writing – review & editing, Investigation, Funding acquisition, Conceptualization. **Hong Yeoul Kim:** Writing – review & editing, Project administration, Investigation. **Se Bok Jang:** Writing – review & editing, Supervision, Project administration, Investigation, Funding acquisition, Conceptualization.

Declaration of competing interest

The authors declare that they have no conflicts of interest with the contents of this article.

Acknowledgements

This study was supported by the Basic Science Research Program through the National Research Foundation of Korea (NRF) funded by the Korean Ministry of Education, Science and Technology (Grant no. 2018R1D1A1B07043701) to S.B.J. and (Grant no. 2016R1D1A1B02011142) to M.S.J. This work was supported by the National Research Foundation of Korea (NRF) grant funded by the Korea government (MSIT) (No. 2021R1C1C2004755) to C.W.H.

Appendix A. Supplementary data

Supplementary data to this article can be found online at https://doi.org/10.1016/j.bbrc.2024.150306.

References

[1] S.A. Krupenko, FDH: an aldehyde dehydrogenase fusion enzyme in folate metabolism, Chem. Biol. Interact. 178 (2009) 84–93.
[2] J.H. Kang, S.-H. Lee, J.-S. Lee, B. Nam, T.W. Seong, J. Son, H. Jang, K.M. Hong, C. Lee, S.-Y. Kim, Aldehyde dehydrogenase inhibition combined with phenformin treatment reversed NSCLC through ATP depletion, Oncotarget 7 (2016) 49397.
[3] S.-Y. Kim, Cancer energy metabolism: shutting power off cancer factory, Biomolecules & Therapeutics 26 (2018) 39.
[4] V. Koppaka, D.C. Thompson, Y. Chen, M. Ellermann, K.C. Nicolaou, R.O. Juvonen, D. Petersen, R.A. Deitrich, T.D. Hurley, V. Vasiliou, Aldehyde dehydrogenase inhibitors: a comprehensive review of the pharmacology, mechanism of action, substrate specificity, and clinical application, Pharmacol. Rev. 64 (2012) 520–539.
[5] M. Yang, K.H. Vousden, Serine and one-carbon metabolism in cancer, Nat. Rev. Cancer 16 (2016) 650–662.
[6] P.B. Rowe, D. Sauer, D. Fahey, G. Craig, E. McCairns, One-carbon metabolism in lectin-activated human lymphocytes, Arch. Biochem. Biophys. 236 (1985) 277–288.
[7] P.M. Tedeschi, E.K. Markert, M. Gounder, H. Lin, D. Dvorzhinski, S. Dolfi, L. L. Chan, J. Qiu, R. DiPaola, K. Hirshfield, Contribution of serine, folate and glycine metabolism to the ATP, NADPH and purine requirements of cancer cells, Cell Death Dis. 4 (2013) e877, e877.
[8] A. Vazquez, E.K. Markert, Z.N. Oltvai, Serine biosynthesis with one carbon catabolism and the glycine cleavage system represents a novel pathway for ATP generation, PLoS One 6 (2011) e25881.
[9] L.N. Zhao, P. Kaldis, The catalytic mechanism of the mitochondrial methylenetetrahydrofolate dehydrogenase/cyclohydrolase (MTHFD2), PLoS Comput. Biol. 18 (2022) e1010140.
[10] P.M. Tedeschi, A. Vazquez, J.E. Kerrigan, J.R. Bertino, Mitochondrial methylenetetrahydrofolate dehydrogenase (MTHFD2) overexpression is associated with tumor cell proliferation and is a novel target for drug DevelopmentMTHFD2 is a novel anticancer target, Mol. Cancer Res. 13 (2015) 1361–1366.
[11] S.A. Krupenko, N.V. Oleinik, 10-formyltetrahydrofolate Dehydrogenase, One of the Major Folate Enzymes, Is Down-Regulated in Tumor Tissues and Possesses Suppressor Effects on Cancer Cells, 2002.
[12] M. Hong, Y. Lee, J.W. Kim, J.S. Lim, S.Y. Chang, K.S. Lee, S.G. Paik, I.S. Choe, Isolation and characterization of cDNA clone for human liver 10-formyltetrahydrofolate dehydrogenase, IUBMB Life 47 (1999) 407–415.
[13] S.A. Krupenko, C. Wagner, Aspartate 142 is involved in both hydrolase and dehydrogenase catalytic centers of 10-formyltetrahydrofolate dehydrogenase, J. Biol. Chem. 274 (1999) 35777–35784.

[14] S.A. Krupenko, C. Wagner, R.J. Cook, Cysteine 707 is involved in the dehydrogenase active site of rat 10-formyltetrahydrofolate dehydrogenase (*), J. Biol. Chem. 270 (1995) 519–522.
[15] P.M.-H. Chang, C.-H. Chen, C.-C. Yeh, H.-J. Lu, T.-T. Liu, M.-H. Chen, C.-Y. Liu, A. T. Wu, M.-H. Yang, S.-K. Tai, Transcriptome analysis and prognosis of ALDH isoforms in human cancer, Sci. Rep. 8 (2018) 1–10.
[16] S. Lee, J.-S. Lee, J. Seo, S.-H. Lee, J.H. Kang, J. Song, S.-Y. Kim, Targeting mitochondrial oxidative phosphorylation abrogated irinotecan resistance in NSCLC, Sci. Rep. 8 (2018) 1–11.
[17] J.H. Kang, S.-H. Lee, D. Hong, J.-S. Lee, H.-S. Ahn, J.-H. Ahn, T.W. Seong, C.-H. Lee, H. Jang, K.M. Hong, Aldehyde dehydrogenase is used by cancer cells for energy metabolism, Exp. Mol. Med. 48 (2016) e272, e272.
[18] F. Jiang, Q. Qiu, A. Khanna, N.W. Todd, J. Deepak, L. Xing, H. Wang, Z. Liu, Y. Su, S.A. Stass, Aldehyde dehydrogenase 1 is a tumor stem cell-associated marker in lung cancer, Mol. Cancer Res. 7 (2009) 330–338.
[19] J. Park, J.-K. Shim, J.H. Kang, J. Choi, J.H. Chang, S.-Y. Kim, S.-G. Kang, Regulation of bioenergetics through dual inhibition of aldehyde dehydrogenase and mitochondrial complex I suppresses glioblastoma tumorspheres, Neuro Oncol. 20 (2018) 954–965.
[20] G.K. Rekha, N.E. Sladek, Inhibition of human class 3 aldehyde dehydrogenase, and sensitization of tumor cells that express significant amounts of this enzyme to oxazaphosphorines, by the naturally occurring compound gossypol, in: Enzymology and Molecular Biology of Carbonyl Metabolism, vol. 6, Springer, 1996, pp. 133–146.
[21] C. Van Poznak, A.D. Seidman, M.M. Reidenberg, M.M. Moasser, N. Sklarin, K. Van Zee, P. Borgen, M. Gollub, D. Bacotti, T. Yao, Oral gossypol in the treatment of patients with refractory metastatic breast cancer: a phase I/II clinical trial, Breast Cancer Res. Treat. 66 (2001) 239–248.
[22] A. Punjani, J.L. Rubinstein, D.J. Fleet, M.A. Brubaker, cryoSPARC: algorithms for rapid unsupervised cryo-EM structure determination, Nat. Methods 14 (2017) 290–296.
[23] E.F. Pettersen, T.D. Goddard, C.C. Huang, G.S. Couch, D.M. Greenblatt, E.C. Meng, T.E. Ferrin, UCSF Chimera—a visualization system for exploratory research and analysis, J. Comput. Chem. 25 (2004) 1605–1612.
[24] P. Emsley, K. Cowtan, Coot: model-building tools for molecular graphics, Acta Crystallogr., Sect. D: Biol. Crystallogr. 60 (2004) 2126–2132.
[25] D. Liebschner, P.V. Afonine, M.L. Baker, G. Bunkóczi, V.B. Chen, T.I. Croll, B. Hintze, L.-W. Hung, S. Jain, A.J. McCoy, Macromolecular structure determination using X-rays, neutrons and electrons: recent developments in Phenix, Acta Crystallogr. D: Struct. Biol. 75 (2019) 861–877.
[26] Y. Tsybovsky, V. Sereda, M. Golczak, N.I. Krupenko, S.A. Krupenko, Structure of putative tumor suppressor ALDH1L1, Commun. Biol. 5 (2022) 3.
[27] D.A. Horita, S.A. Krupenko, Modeling of interactions between functional domains of ALDH1L1, Chem. Biol. Interact. 276 (2017) 23–30.
[28] R.L. Kisliuk, Folate Biochemistry in Relation to Antifolate Selectivity, Antifolate Drugs in Cancer Therapy, 1999, pp. 13–36.
[29] N.I. Krupenko, M.E. Dubard, K.C. Strickland, K.M. Moxley, N.V. Oleinik, S. A. Krupenko, ALDH1L2 is the mitochondrial homolog of 10-formyltetrahydrofolate dehydrogenase, J. Biol. Chem. 285 (2010) 23056–23063.
[30] X. Li, L. Wan, J. Geng, C.-L. Wu, X. Bai, Aldehyde dehydrogenase 1A1 possesses stem-like properties and predicts lung cancer patient outcome, J. Thorac. Oncol. 7 (2012) 1235–1245.
[31] J. Fan, J. Ye, J.J. Kamphorst, T. Shlomi, C.B. Thompson, J.D. Rabinowitz, Quantitative flux analysis reveals folate-dependent NADPH production, Nature 510 (2014) 298–302.